Study of new types of dynamic interactions in power systems with mixed conventional and renewable generation

Pamela Zoghby, Bogdan Marinescu, Antoine Rossé

Study of new types of dynamic interactions in power systems with mixed conventional and renewable generation

Pamela ZOGHBY*

EDF R&D / Ecole Centrale Nantes, LS2N
France
pamela.zoghby@edf.fr

Bogdan MARINESCU

Ecole Centrale Nantes, LS2N
France
bogdan.marinescu@ec-nantes.fr

Antoine ROSSÉ
Grégoire PRIME

EDF R&D
France
antoine.rosse@edf.fr

SUMMARY

In the context of the evolving energy mix of power systems, marked by the growing integration of renewable energy sources and battery energy storage systems (BESS), the dynamics of power systems are undergoing significant changes. In such systems, dynamic couplings between inverter-based resources (IBRs) and synchronous machines (SM) may occur, leading to stability issues. Stability concerns may also emerge due to communication delays between external control loops and inverter's reference input, interacting with both the inverter's primary frequency control and the frequency meter (FM) used to measure the grid's electrical frequency.

The current paper analyses and studies these phenomena on a use-case based on a French island power system. This system may experience oscillations among its generation sources, causing concerns for the grid operator. Therefore, there is a need for comprehensive studies to highlight the phenomena that could compromise stability and operational safety, especially considering the significant number of new renewable energy and BESS projects that are currently under development.

For this purpose, an inherited simple and sufficient conceptual benchmark is used with some adaptations to model the island power system. This benchmark, composed of an inverter, a synchronous machine, and an equivalent dynamic grid model, has been linearized around various operating points, and modal analysis applied to detect and analyse all the oscillation modes. Also, participation factors are used to gain insights on the type of each mode. Through modal analysis, sensitivity studies are conducted to assess the impact of key parameters on the damping of newly identified oscillation modes. The linearized benchmark is validated through nonlinear time-domain EMT-based (electromagnetic transient) simulations using commercial EMT simulation tools.

Two new modes of oscillation are detected in addition to the traditional inter-area mode and average frequency mode. The first one is caused by interactions between the synchronous machine and the inverter and is called *coupling mode*. The second one, called *control delay mode*, is mainly due to an interaction between the communication delay and the inverter's primary frequency control. Finally, a Power System Stabilizer (PSS) has been tuned and installed on the SM to damp the inter-area mode, and a Power Oscillation Damping (POD) controller added to the inverter's power control loop has been proposed and proven to be effective in damping the average frequency mode.

KEYWORDS

Conceptual Benchmark, Modal Analysis, Interactions, Oscillation Modes, Synchronous Machines, Inverter-based Resources, Power Oscillation Damping, Island Power System.

1 INTRODUCTION

Power oscillations are a persistent concern that threaten the stability and reliability of power systems. These oscillations can induce frequency instabilities, prompting protective relays and activating load shedding, potentially resulting in widespread blackouts in extreme cases. Many worldwide power system collapses have been reported over the past decades such as the Western Systems Coordinating Council on August 10, 1996, caused by an unstable 0.25 Hz inter-area mode [1].

Power oscillations can also impact voltage stability, potentially leading to voltage collapse. Additionally, oscillations with frequencies close to the natural frequencies of system components, such as rotating machines, have the potential to cause significant mechanical and electrical damage to equipment and may result in loss of synchronism between generators and the grid. Historically, these oscillations have been investigated in traditional power systems where synchronous machines (SMs) played a predominant role as electricity producers [2].

As power systems transition towards cleaner energy production, SMs are progressively being replaced by Inverter-Based Resources (IBRs) such as solar photovoltaic (PV), wind turbines and battery energy storage systems (BESS). IBR dynamics have a broad range spanning from high switching frequencies, rapid controls (inner loops and Phase Locked Loops (PLL)) to slower dynamic ranges, with outer loops such as power and voltage control with communication delays. Therefore, in a mixed power system with both traditional and renewable generation, diverse time-scale dynamics may interact, giving rise to new oscillatory modes in addition to classical well-known power oscillations such as inter-area modes [3].

In power system stability analyses, communication delays are often neglected for the sake of simplicity. However, recent studies have begun to examine their impact on power systems, exploring aspects such as their influence on the subsynchronous interaction controller in wind farms [4] and their effect on Power System Stabilizer (PSS) [5]. In [6] authors study the small-signal stability of a two-area power system experiencing inter-area oscillations with a damping controller subjected to two different and independent latencies. However, the system considered in their study is traditional including only SMs. In [7] the performance of frequency regulation in Photovoltaic Power Plants (PVPP) is analysed under various time delay scenarios. As delays increase, the capability of PVPP to stabilize the grid through primary frequency regulation is weakened.

Various studies in the literature have studied coupling modes due to interactions between a SM and an inverter, such as in [3], where the authors focus on the small-signal stability analysis of low inertia power systems with detailed modelling of the components. Key parameters, including transmission line length and IBR penetration level, are explored to identify their effects on small-signal stability. Nevertheless, control delays are not considered, and the system examined is a simplified academic representation that may not accurately depict a real power system.

These challenges can emerge not only in interconnected power systems, but also in isolated island systems, where the transition to renewable energy is occurring at an accelerated pace. This paper focuses on the study of the stability of a real French island power system prone to power oscillations, with a focus on the impact of new SM and IBR projects that are currently under development and will be connected to the grid in the coming years. In this context, a methodology is employed to facilitate reduced-order modeling, enabling the study of dynamic interactions among specific elements of the grid. This approach utilizes a conceptual benchmark derived from [8], with necessary modifications to accurately reflect the characteristics of the island system under investigation. New types of modes are identified and analysed using modal analysis and participation factors. Also, sensitivity analyses are conducted to detect key parameters influencing the stability of the power system. Finally, corrective measures are proposed to improve the damping of critical oscillation modes.

The rest of this paper is organized in the following manner: Section 2 explains how the parameters of the benchmark are tuned to accurately represent the system of interest. In Section 3, modal analysis is applied to the linearized system to elucidate the key oscillation modes of the system. Section 4 presents sensitivity analyses by varying key parameters and their impact on the modes of oscillation. Section 5 proposes PSS and Power Oscillation Damping (POD) controllers to improve the damping of key oscillation modes. Finally, Section 6 presents the conclusion and future works.

2 A CONCEPTUAL BENCHMARK FOR THE STUDY OF A REAL FRENCH ISLAND POWER SYSTEM

For a comprehensive analysis, study, and quantification of different modes of oscillation and their sensitivity to communication delays in a power system with IBRs and SM, the benchmark introduced in [8] is used in this paper to study a French island power system. The benchmark, depicted in Figure 1, is designed with simplicity for ease of analysis and interpretation while still adequately capturing the system's interactions and resulting oscillation modes. Moreover, it serves as a multi-source methodology capable of representing any real power system, specifically designed to capture interactions between specified dynamic elements, as exemplified in the island power system discussed here. It offers a balanced approach between the simplified two-source systems often found in literature, such as SM vs IBR or IBR vs Infinite-bus, and the more detailed models of the studied power systems.

The power system of interest is divided into two areas. An area in the East contains most of the grid's load and production comprising six generators employing various technologies such as hydraulic and gas turbines, each equipped with power and voltage regulation capabilities. Within the benchmark, the eastern area is aggregated into a single unit, called the EquGrid block, which functions as a grid equivalent, capturing the dynamic behaviour of the six eastern generators and the total load. In the other area, located in the West, a power generation site containing a SM and an IBR is connected to the 20 kV medium-voltage grid, as illustrated in Figure 1. These generation units in the western area represent new projects that are currently under development and are expected to be connected to the grid in the coming years. Currently, generation is centralized in the East with no production in the West, and the system of interest therefore exhibits no East-West inter-area oscillations in its current configuration. However, with new generation units arriving in the West in the coming years, new inter-area modes are expected to appear, as it will be demonstrated further in this paper through modal analysis. The two areas are connected through a long-distance 90 kV high-voltage transmission line represented by Z_{cc}.

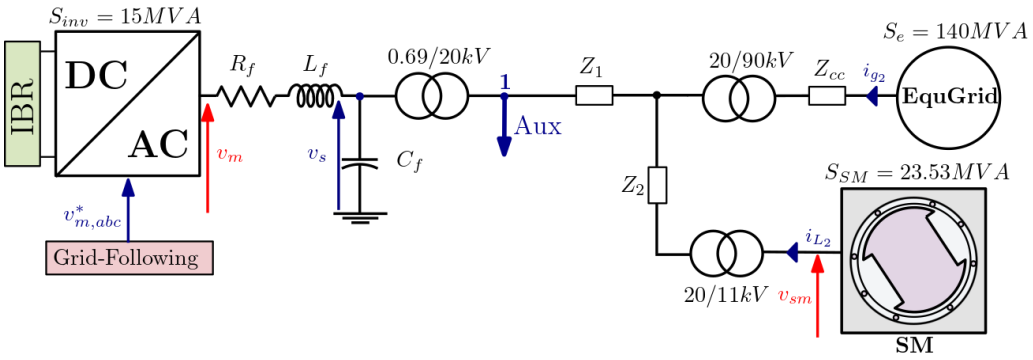

Figure 1 : Benchmark adapted to represent the French island power system.

Compared to the benchmark in [8], a load has been positioned at node 1 to represent typical auxiliary consumptions (e.g., heating, air conditioning, control units, ...) at the IBR's output. The medium-voltage grid's transmission lines' nominal voltage is fixed at 20 kV. A detailed grid model including the SM, voltage, and speed regulations of each individual generation unit in the eastern area was developed and implemented in a commercial EMT simulation software. Next, the future generation units in the western region were incorporated into the complete model of the island power system. Based on the data of this detailed grid model, the corresponding line impedance values were determined for the benchmark as follows: $Z_1 = Z_2 = 0.12 + j\,0.1\,\Omega/km$ and $Z_{cc} = 0.14 + j\,0.4\,\Omega/km$ with the respective distances $l_1 = l_2 = 15\ km$ and $l_{cc} = 200\ km$. The benchmark can be easily adapted to represent different types of power systems, from large, interconnected networks to small, isolated microgrids, by simply adapting the parameters such as nominal powers, line voltages and impedances.

In the benchmark, a detailed model of a classical salient pole SM with the dynamics of the stator and dampers, and equipped with an exciter, prime mover and governor simplified to the first order inherited from [8] has been used to represent the conventional generation unit in the medium-voltage grid. The IBR is a Voltage Source Converter (VSC) represented by an ideal average model neglecting the high switching frequencies, with a Proportional-Integral (PI) d-q frame current controller and a typical PI-

based PLL structure, as detailed in [8], operating in grid-following mode. The inverter's current control loop response time is set to a typical value of 10 ms. The main difference compared to the structure proposed in [8] concerns the placement of the primary frequency control, which is moved to the inverter's external power control loop as detailed later in this paper.

2.1 Equivalent Grid Model

The dynamics of the equivalent grid model employed in [8] exclusively account for instantaneous primary frequency regulation and the auto-adaptive regulation of the load. However, this simplified dynamic representation may not be accurately representative of today's island power systems in which primary frequency control is generally ensured by either BESS, conventional power plants with synchronous machines (mainly hydro or thermal), or a mix of both.

Since the western area of the studied power system represents generation units that are currently under development and not yet in service, the equivalent grid model (EquGrid block in Figure 1) represents the global dynamics of the island grid as it currently exists today. Therefore, the dynamics of the EquGrid can be tuned based on the current observed dynamic behaviour of the grid. Figure 2 shows the measured frequency response of the island system being studied following a sudden load variation of $\Delta P = 3$ MW within the grid. This frequency response has been approximated by an equivalent second-order transfer function represented in equation (1) using commercial system identification tools.

$$H_i(s) = \frac{0.132\ s + 0.109}{s^2 + 0.26\ s + 1.12} \tag{1}$$

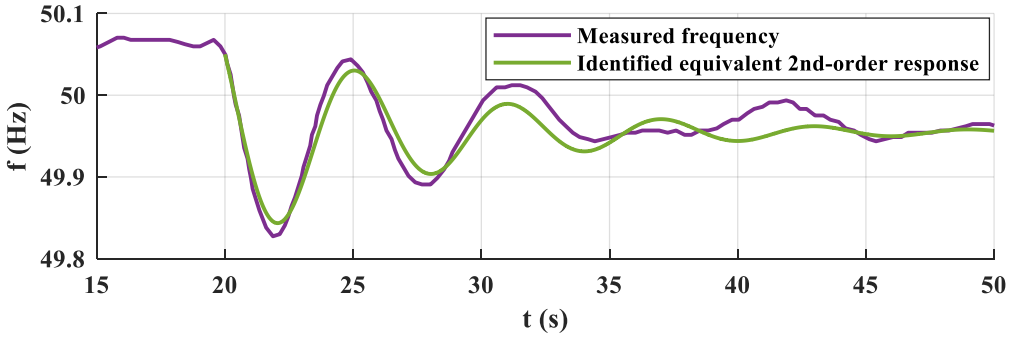

Figure 2: Frequency response of the island power system after a sudden load variation of 3MW.

To better represent the real global frequency dynamics of the grid illustrated in Figure 2, the equivalent grid dynamic model proposed in [8] has been improved by introducing a lead-lag filter in the feedback loop of the swing equation, as depicted in Figure 3. With this structure, the equivalent grid's dynamic response becomes a second-order system whose parameters can be calculated to represent the measured dynamics of the grid as illustrated in Figure 2.

P_{EG} is the active power generated within the grid and P_l is the power consumed by the system's loads. The transfer function $H_{EquGrid}$ having the frequency variation as an output and the power variation as an input has been developed and presented in equation (2).

$$H_{EquGrid}(s) = \frac{\frac{1}{2H_e}\ s + \frac{1}{2H_eT_{e2}}}{s^2 + \left(\frac{1}{T_{e2}} + \frac{K_gT_{e1}}{2H_eT_{e2}}\right)s + \frac{K_g}{2H_eT_{e2}}} \tag{2}$$

By matching the two transfer functions in equations (1) and (2), the parameters of the equivalent grid model are determined and provided in Table I. The step response of the transfer function $H_{EquGrid}$ is also presented in Figure 2, showing that the equivalent grid model accurately reproduces the main oscillatory behaviour observed on the actual power system.

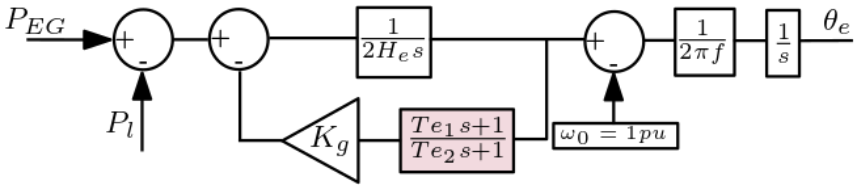

Figure 3: Equivalent Grid block diagram.

Table I: Equivalent grid's parameters.

H_e **(s)**	3.78	T_{e1} **(s)**	-0.5056
K_g **(pu)**	10.24	T_{e2} **(s)**	1.21

With this representation, the network load in the benchmark system is modelled within the equivalent grid model, whose dynamic response includes both the aggregated dynamics of the generation units and the frequency-dependence of the load. Also, the IBR's auxiliary consumption is modelled as constant impedance. However, these models may present some limitations as they do not account for certain phenomena such as voltage dependencies or potential nonlinearities of the loads.

2.2 External Power Loop

In real-world industrial projects, the inverter and its internal control, obtained from the manufacturer, typically presents itself as a black box – a sealed system without any accessible interface to the internal control loops. In terms of active power control, the interfaces of commercial inverters are often limited to an active power setpoint P_{ref}. Common industrial practice for BESS integrators is to implement power control algorithms including primary frequency control within an external controller (sometimes called Power Management System (PMS), Real-Time Controller, or other terms), which will calculate the power setpoint and communicate it to the inverter via a telecommunication link using a communication protocol such as Modbus, IEC-104, IEC-61850, DNP3, etc.

With this typical architecture, an inherent delay is introduced by the communications link between the external power control loop and the inverter's control input P_{ref}, as illustrated in Figure 4. This paper proposes to consider a typical BESS control architecture in which the external power loop, designed to regulate the IBR's active power at the grid connection point by compensating losses and auxiliary power consumption, is composed of a PI controller with a feed-forward on the power setpoint $(P_0 - P^*)$.

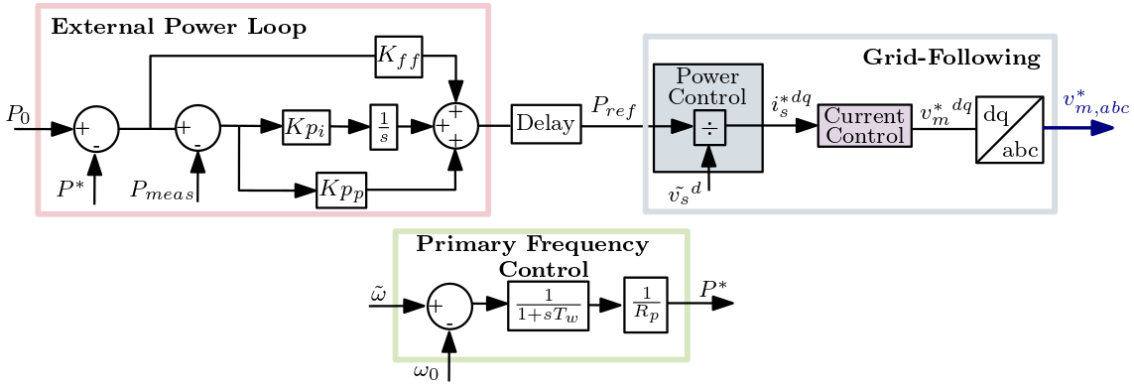

Figure 4: Block diagram of the external power loop, primary frequency control and the grid-following control.

The primary frequency control term P^* is added to the base setpoint P_0. A low-pass filter of time constant $T_w = 100\ ms$ is included to reduce frequency oscillations as proposed in [9]. The droop gain R_p is adjustable, allowing for sensitivity analyses in the subsequent sections. The measured frequency $\tilde{\omega}$ is determined by a dedicated frequency meter (FM) modelled using a PLL. Note that the FM's PLL is independent of the inverter's internal control PLL, as the FM represents an independent equipment that is separate from the inverter hardware.

2.3 Communication Delay

Communication delays can be linearized using the Padé approximation [10] for modal analysis studies. The appropriate order of the Padé approximation required to accurately represent the dynamic response of the nonlinear system depends on the system's characteristics.

Figure 5 displays an illustration of the system's response to a 0.05 pu step of the inverter's setpoint P_0 for various orders of the Padé delay approximation up to the fourth order, compared with the time-domain response of the detailed nonlinear model using a pure delay. The fourth-order Padé approximation provides the closest response to the pure delay and is therefore chosen to model the delay in the modal analysis study. Higher order Padé approximations could also be considered, however each increase in order adds additional states and complexity to the linearized model. The fourth order was found to be an appropriate compromise between accuracy and complexity.

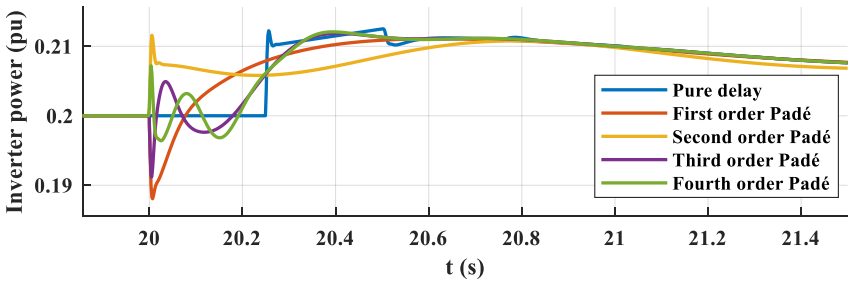

Figure 5: The power response measured at the output of the inverter after a step of 0.05 pu applied to P_0.

3 MODAL ANALYSIS RESULTS

To investigate oscillation modes arising from interactions between IBRs and SM, as well as the impact of communication delays, external power loops, primary frequency control and PLL, a modal analysis approach is employed in conjunction with nonlinear time-domain simulations. While nonlinear time-domain simulations cannot capture highly damped oscillation modes and offer limited insights into mode types, modal analysis is well adapted to address these constraints. The method applied involves developing the differential-algebraic equations of every component in the dq frame taking into account the EMT dynamics as in [9]. The full benchmark written in the form of DAE (Differential Algebraic Equations) is then linearized around an operating point [2][11] and put into state-space form as in (3).

$$\dot{x} = Ax \tag{3}$$

While linearization tools exist in some commercial modelling software, these tools present some limitations such as employing numerical methods, which may lack transparency regarding the specific details of the methodology and being limited to linearizing only phasor (RMS) dynamics. For a more rigorous approach that preserves EMT dynamics, the authors have opted for manually writing the system equations element by element. As to the author's knowledge, no existing commercial tools offer model linearization with this level of detail and fidelity to EMT dynamics.

Once the equations of the system's individual components have been assembled and the full system expressed in state-space form as in (3), each complex conjugate eigenvalue of matrix A expressed in the form $\lambda_i = \sigma_i \pm j\omega_i$ indicates an oscillatory mode. The real part σ_i gives an indication about the stability of the mode; if σ_i is positive, the eigenvalue is in the right half-plane and the mode is unstable. If σ_i is negative, the eigenvalue is in the left-half plane and the mode is stable. The imaginary part represents the frequency of the mode. The damping of the mode ζ_i can be calculated according to equation (4).

$$\zeta_i = \frac{-\sigma_i}{\sqrt{\sigma_i^2 + \omega_i^2}} \tag{4}$$

Also, it is possible from matrix A to discern mode types by evaluating the participation factors and to conduct sensitivity analyses to highlight key parameters influencing the modes. Moreover, mode shapes

can be calculated and plotted, and they are used to assess how each state variable is affected when a particular mode is excited. The accuracy of the linearized model has been verified by comparing it with nonlinear EMT simulation as detailed in [8].

Table II presents the key identified oscillation modes of the system, obtained considering a controller time delay value of 100 ms and a droop value Rp set at 1%.

Table II : Relevant modes' frequency, damping and participating factors obtained from the modal analysis.

Mode	$\lambda = \sigma \pm j\omega$	Frequency (Hz)	Damping (%)	Main Participation Factors
Inter-area mode	-0.45 ± j9.13	1.45	4.9	$\Delta\omega_{SM}, \Delta\theta_{SM}, \Delta\theta_e, \Delta\omega_e$
Average Frequency mode	-0.46 ± j1.38	0.22	31.3	$\Delta\omega_{SM}, \Delta P_{gov}, \Delta\omega_e, \Delta T_e, \Delta w_{filt}$
Control delay mode	-1.85 ± j32.8	5.22	5.7	$\Delta\gamma_{PLL}, \Delta\theta_{PLL}, \Delta\omega_{filt}, \Delta\gamma_{FM}, \Delta D_1, \Delta D_2, \Delta D_3, \Delta D_4$
Coupling mode	-205 ± j440	70	42	$\Delta vsdq, \Delta isdq, \Delta\gamma curr_{dq}, \Delta\Psi_{dq}$

As shown in Table II, the conventional inter-area mode [2] between the SM and the EquGrid is clearly identified, as it involves states relating to the SM and the EquGrid's swing equations. This identification is confirmed by the mode shapes in Figure 6 indicating that the speeds of the SM and EquGrid are in anti-phase [11]. Note that this mode is not well damped, and therefore the addition of a PSS on the SM may be necessary to enhance its damping as explained further in section 5.

The average frequency mode, characterized by a very low frequency, plays a crucial role in regulating the power system's global frequency [12] [13]. The participating factors in this mode include the SM's speed ($\Delta\omega_{SM}$), the governor-related state of the SM (ΔP_{gov}), the state associated with the dynamics of the EquGrid ($\Delta\omega_e, \Delta T_e$) and the state linked to the filter of the inverter's primary frequency control (Δw_{filt}). The mode shape depicted in Figure 6 confirms that the rotor speed of the SM and the equivalent grid oscillate coherently, confirming that this mode regulates the frequency of the entire system [12].

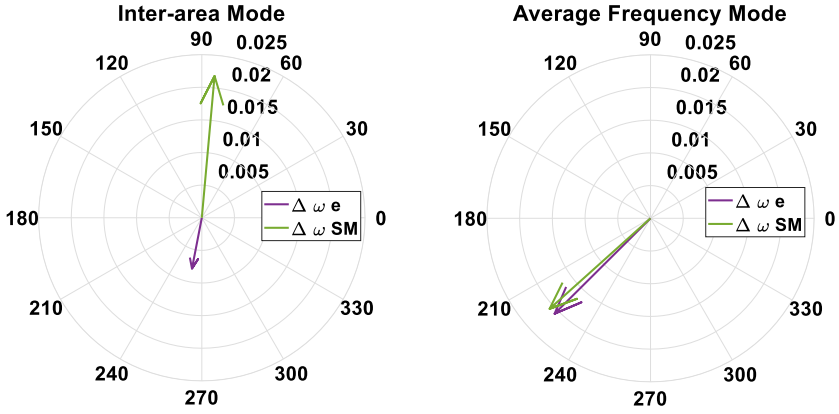

Figure 6: Mode Shapes.

The control delay mode is a newly identified oscillatory mode, introduced by the presence of the communication delay. It involves participating factors such as the internal PLL's states ($\Delta\gamma_{PLL}$, $\Delta\theta_{PLL}$), Δw_{filt}, the state related to the frequency meter ($\Delta\gamma_{FM}$) and the states associated with the approximation of the delay with the fourth-order Padé function (ΔD_1, ΔD_2, ΔD_3, ΔD_4). Figure 7 shows that this oscillation disappears when the model is simulated without the delay, thus confirming that this mode is caused by the delay.

The coupling mode arising from the interaction between the SM and the inverter manifests at a higher frequency than the others. The states concerned are the voltage and current in the inverter's filter respectively ($\Delta vsdq$, $\Delta isdq$), the states of the inverter's current loop PI controller ($\Delta\gamma curr_{dq}$) and the fluxes of the SM ($\Delta\Psi_{dq}$).

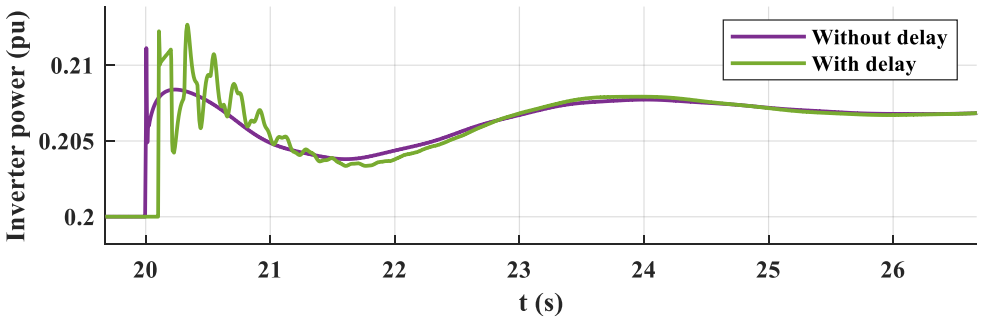

Figure 7: inverter's power after a setpoint step of 0.05 pu of P_0.

To validate the oscillation modes obtained from the benchmark through modal analysis against the real island power system, time-domain simulations were performed using the complete island power system model described in Section 2, employing the same configuration of the western units that yielded the results of Table II. The results of these simulations, presented in Figure 8, show a clear inter-area oscillation between the SM of the western area against the three largest generators units of the eastern area, at a frequency of approximately 1.4 Hz with low damping, and a global average frequency oscillation at approximately 0.22 Hz which is well damped after a couple of oscillations. These results are consistent with the modal analysis results obtained with the linearized benchmark presented in Table II, thus validating the use of the dynamic grid equivalent and model reduction approach of the benchmark for correctly assessing the system oscillation modes in a reduced-order modelling.

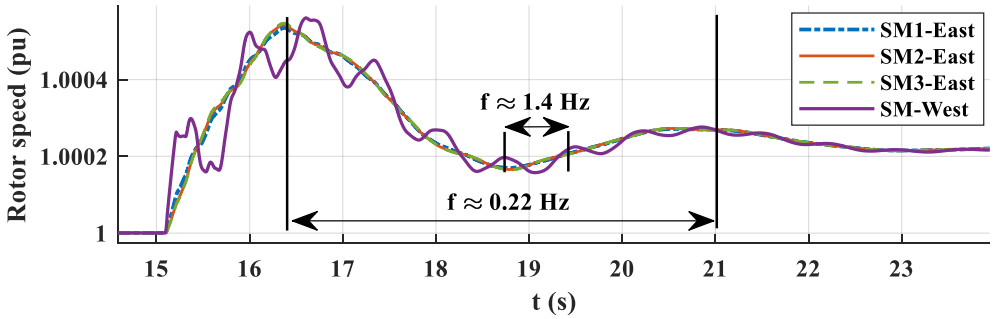

Figure 8: SM's rotor speed after a step change of the inverter's power setpoint of 0.05 pu.

In the following section, sensitivity analyses are conducted to explore the impact of key parameters on the identified oscillation modes. Some grid operators require manufacturers to provide detailed block diagrams of the IBR's control, allowing for possible adaptation of the linearized control model within the proposed benchmark, in alignment with the objectives of the C4.71 CIGRE Working Group [14], which aims to provide guidance on small-signal modelling in power systems with high shares of IBR. However, the control system of the inverter is often unknown, making the generic IBR model potentially unrepresentative. Nevertheless, modern inverters typically have high-bandwidth internal controllers with minimal interference with slower external controllers. Notably, the participation factor analysis suggests that only the coupling mode may be significantly influenced by variations in the inverter's internal control structure.

4 SENSITIVITY ANALYSIS

The modes of oscillation are graphically represented in the complex plane, providing insights into their behaviour as the droop, the communication delay and the topology of the grid are systematically varied within a suitable range. The diagonal bars in the complex plane indicate the damping factor ζ_i. When a mode shifts to the left, it indicates an increase in damping, while a shift to the right means a decrease in damping.

4.1 Sensitivity to the droop R_p

The value of the inverter's droop control has been varied from 1% to 5% to evaluate the influence of the primary frequency control gain on system stability. The results of the modal analysis are shown in

Figure 9. A reduction in R_p from 5% to 1% enhances the damping of the average frequency mode [13], improving it from 17% to 31%. On the other hand, the damping of the control delay mode decreases drastically from 41% to 5.7% with the same adjustment in R_p. In contrast, the analysis also shows that the droop control gain has little effect on the inter-area mode.

The coupling mode's damping increases from 41% to 61% when R_p is increased. While the coupling mode is influenced by the droop, its damping remains relatively high compared to the lower-frequency modes, which are prone to instability and require more careful attention.

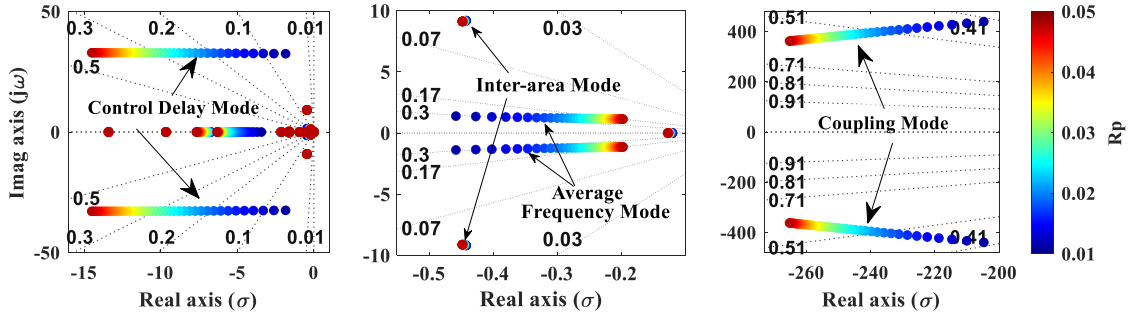

Figure 9: The displacement of the eigenvalues in the complex plane when Rp is varied.

The modal analysis sensitivity study can be applied to system parameter design with regards to the overall system dynamics. For example, when choosing the value of the IBR's droop setting, a compromise must be reached based on the damping of the average frequency mode and that of the control delay mode. For the island power system treated in this paper, a range of $\boldsymbol{R_p}$=3% up to $\boldsymbol{R_p}$=5% is appropriate, as these parameter values ensure a damping of at least 17% for each of the critical modes, which is sufficient for ensuring robust system stability.

4.2 Sensitivity to the communication delay time constant T

To model various possible system architectures, either with fast communication buses or those featuring low sampling rates or multiple intermediary communication interfaces (i.e., a real data transmission chain), the communication delay time constant T has been varied within the range of 10 ms to 400 ms. The droop control setting R_p is fixed at the initial value of 1% for this sensitivity analysis.

As depicted in Figure 10, the damping of the control delay mode decreases as the communication time delay becomes longer for values of T less than 150 ms. For values greater than 150 ms, the trend is reversed, and the damping of the mode increases as the delay becomes longer. Thus, the minimum damping value is obtained for a delay of around 150 ms. Similar behaviour is observed on the inter-area mode, but this time the damping decreases to reach almost 3.5% for T = 300 ms, then increases to 4.2% for T = 400 ms. The average frequency mode has an opposite trend compared to the inter-area mode.

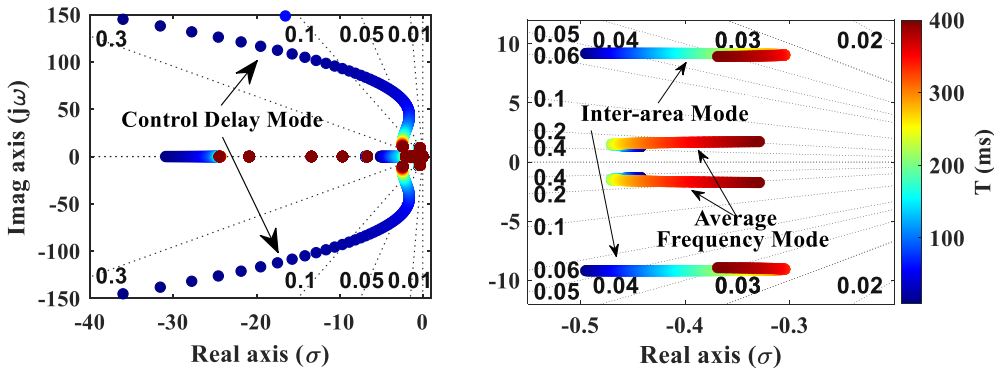

Figure 10: The displacement of the low-frequency eigenvalues in the complex plane when T is varied.

The coupling mode's damping is minimally affected by the communication delay; therefore, the corresponding graphical results are not presented here.

4.3 Sensitivity to the grid topology

While the power system's geographical distances are fixed, operations such as line reinforcement (e.g., adding transmission lines in parallel) can modify the equivalent electrical distance by altering the impedance between two system points.

To evaluate the impact of different grid topologies on the stability of the oscillation modes, different grid strengths have been examined by adjusting the electrical distance l_{cc} between the western area and the equivalent grid in the East.

Figure 11 illustrates that the damping of both the control delay mode and the coupling mode decreases with a weaker grid (for higher l_{cc}) while the damping of the inter-area mode and the average frequency mode remain relatively unchanged.

The findings resulting from the various modal sensitivity analyses conducted in this paper hold significance for system operators, as they highlight the fact that simplified conventional studies such as IBR vs an infinite bus, neglecting SMs dynamics and/or communication delays, may not be sufficient to correctly assess system stability and control risks.

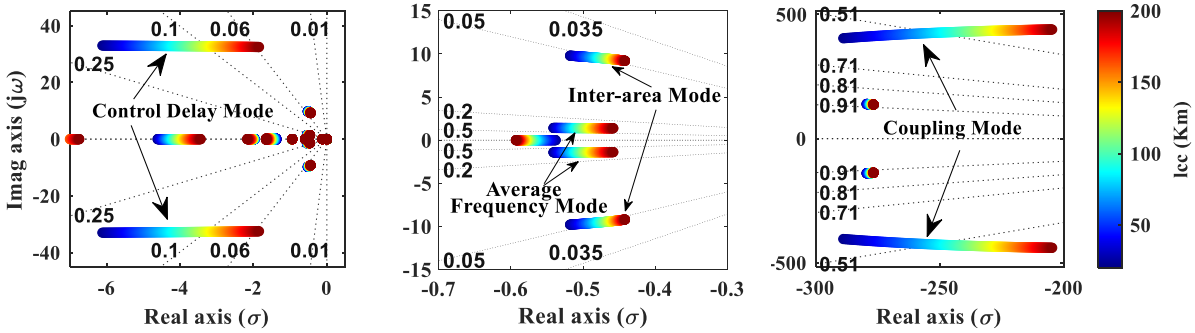

Figure 11: The displacement of the low-frequency eigenvalues in the complex plane when the distance l_{cc} to the equivalent grid is varied.

5 POWER OSCILLATION DAMPING

As mentioned in section 3, the inter-area mode is not well-damped, therefore a PSS installed on the SM may be necessary in this case. A typical PSS structure shown in equation (5) has been used and tuned using the method based on the angle of residues obtained from the modal analysis as described in [15]. The general concepts, performance objectives, tuning concepts and practical considerations of a PSS can be found in [16] [17] [18].

$$\frac{V_{stab}(s)}{\omega(s)} = 20 \ \frac{10\,s}{1+10\,s} \ \frac{1+0.147\,s}{1+0.074\,s} \ \frac{1+0.147\,s}{1+0.074\,s} \tag{5}$$

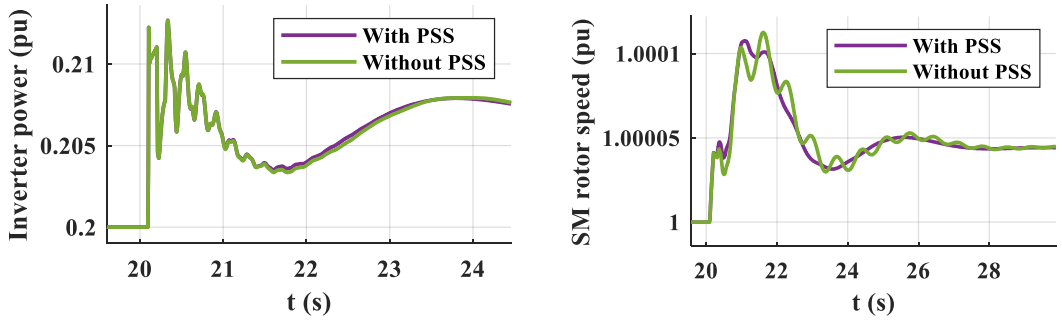

Figure 12: Inverter's active power and the SM's speed responses with and without a PSS obtained on the nonlinear model.

The modal analysis results show that the damping of the inter-area mode increased from 4.9% to 13% after the installation of the PSS, while the control delay mode and the average frequency mode are insensitive to the PSS. These results are confirmed by the nonlinear time-domain simulations presented in Figure 12, which show that the inter-area oscillations visible on the SM's speed are improved thanks to the addition of the PSS on the SM, while the oscillations of the control delay mode visible on the inverter's active power are unaffected by the SM's PSS.

In the preceding sections of this paper, it was assumed that the IBR participates in primary frequency control. The use of BESS for providing primary frequency control in power systems is becoming increasingly widespread. However, for BESS to provide primary frequency control, it is necessary to have a certain dedicated energy storage capacity. For instance, if there is a long-lasting low frequency deviation, the BESS must have sufficient charge to supply power to the grid for the duration of the frequency deviation. On the other hand, the BESS must have sufficient available capacity to be able to charge for the duration of a long-lasting high frequency deviation.

In many large power grids such as the European Continental Network, automatic secondary frequency control mechanisms regulate the frequency to its nominal value, typically within 15 minutes [19], such that long-lasting frequency deviations are limited and thus energy capacity requirements for primary frequency control are not excessive.

However, the French island network considered in the present study does not yet have automatic secondary frequency control, as this function is performed manually by grid operators by modifying power setpoints of the generation units. Consequently, the average grid frequency is not necessarily equal to the nominal frequency, and long-lasting frequency deviations can occasionally last several hours. For a BESS to perform primary classical frequency control on this network, a high energy capacity may therefore be required, thus representing higher investment costs.

To surpass this capacity constraint for primary frequency control by BESS, an alternative control based on a typical POD structure, shown in Figure 13, is proposed to provide dynamic frequency support with the IBR without the high energy capacity constraints (i.e., instead of primary frequency control). While PODs are typically implemented in IBRs to mitigate power oscillations such as inter-area oscillations, in the studied use-case, since the inverter states do not participate in the inter-area mode (see Table II), a POD implemented within its control will be ineffective for inter-area oscillation damping. However, the inverter does participate in the average frequency mode as indicated by the participation of the state Δw_{filt}, which is within the inverter's control. Therefore, the implementation of a POD in the inverter can be useful for damping the average frequency mode, thus limiting the amplitude of frequency oscillations, and potentially avoiding frequency-based load shedding in case of large network disturbances.

Since the high-pass filter in the POD eliminates the steady-state frequency deviation component, the long-lasting frequency deviations no longer imply long charge or discharge phases of the BESS as the POD signal's value will stabilize to zero as shown on the inverter's power response in Figure 13. This enables the POD to act during the transitional period due to variations in the frequency after the occurrence of a certain disturbance.

In addition to BESS, the proposed POD may also be compatible with other IBRs such as wind turbines that can exploit the inertia of the rotational mass in the turbine as a limited energy resource, similarly to services such as "synthetic inertia" or dynamic frequency support that already exist [20].

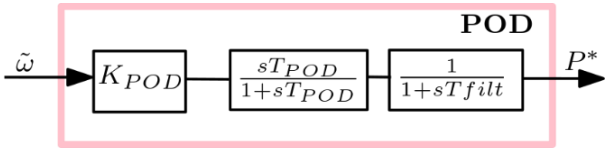

Figure 13: Power Oscillation Damping controller used to stabilize frequency oscillations.

The proposed POD thus enables IBR to provide oscillation damping despite being energy limited. To illustrate this, the primary frequency control in Figure 4 has been replaced by the POD filter within the IBR's power control loop in the benchmark system to conduct modal analysis and assess its effects on

the modes of oscillation. As shown in Figure 13, the POD uses the grid frequency obtained from the frequency meter as an input and P^* as an output. A low-pass filter with a time constant of $T_{filt} = 0.2\ s$ is employed to supress the high frequencies and T_{POD} is set to 5 s. A sensitivity analysis is conducted to study the impact of the POD parameters on frequency damping by varying the gain K_{POD} from 0 to 500 pu as illustrated in Figure 15.

Time-domain simulations and modal analysis results in Figures 14 and 15 show that the damping of the average frequency mode significantly improves from 12% to 30% upon implementing the POD controller without adversely affecting other modes. In particular, the results in Figure 14 show that the frequency nadir can be notably improved thanks to the proposed POD in case of significant grid disturbances.

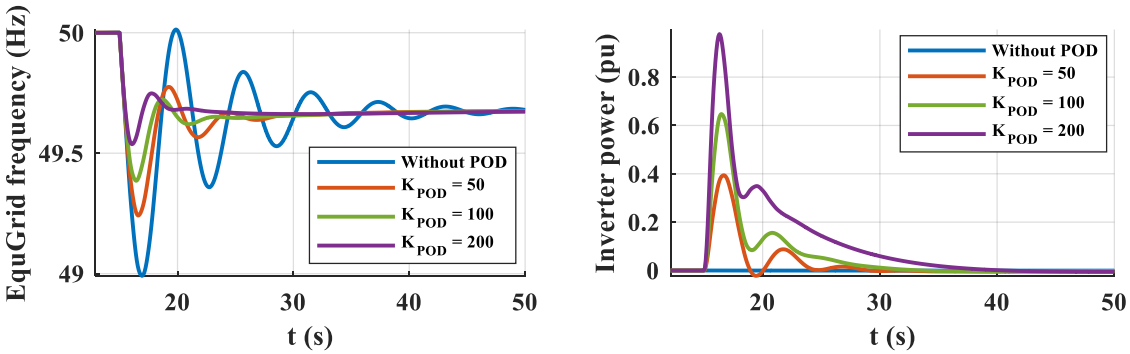

Figure 14: Time-domain simulations showing the frequency oscillations following a load imbalance for different K_{POD} gains.

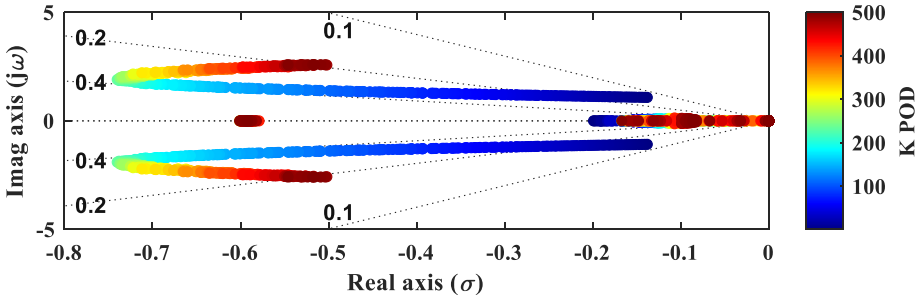

Figure 15: Sensitivity of the average frequency mode to the gain K_{POD}.

6 CONCLUSION

This paper focuses on the study the dynamic stability of a French island power system that includes mixed IBR and SM-based generation in its power production. A conceptual benchmark has been adapted to represent this real-word scenario, and modal analysis based on the linearized model has been employed to identify potential new modes of oscillations that could affect the system's stability.

Through examining the participation factors, two new types of modes have been detected including the coupling mode due to the interaction between the SM and the inverter, and the control delay mode due to an interaction between the communication delay and the primary frequency control. Additionally, the traditional inter-area mode and average frequency mode have been detected and analysed.

Sensitivity analyses have revealed the impact of droop values, communication delay time constant, and grid strength on oscillation modes. To mitigate the damping of the inter-area mode, a PSS has been tuned utilizing the residues technique on the linearized model of the benchmark and subsequently implemented on the SM. Finally, a POD controller implemented on the inverter has been suggested to damp the average frequency mode as an alternative to primary frequency control. Its effectiveness has been shown on the benchmark.

While the proposed benchmark structure presents some limitations, such as the inability to study dynamic interactions between different IBR, it is sufficient to capture a wide range of interactions within mixed SM and IBR power systems. For more specific interaction studies, adaptations such as the addition of extra SM or IBR units for specific interaction studies can be considered.

Future studies will focus on grid-forming controls and their impact on system stability, using the same framework with the adapted linearized benchmark system and modal analysis techniques.

BIBLIOGRAPHY

[1] V. D. Le and E. Al, "A novel approach for determining optimal number and placement of static var compensator device to enhance the dynamic performance in power systems," *Electr. Eng.*, vol. 100, no. 3, pp. 1517–1533, 2018.

[2] P. S. Kundur, "Power System Stability and Control Volume I," *McGraw-Hill, Inc*. pp. 1–600, 2004.

[3] L. Ding and et al, "Comparative Small-Signal Stability Analysis of Grid-Forming and Grid-Following Inverters in Low-Inertia Power Systems Preprint Comparative Small-Signal Stability Analysis of Grid-Forming and Grid- Following Inverters in Low-Inertia Power Systems," *IEEE Ind. Electron. Soc.*, 2022.

[4] M. Ghafouri, U. Karaagac, I. Kocar, Z. Xu, and E. Farantatos, "Analysis and Mitigation of the Communication Delay Impacts on Wind Farm Central SSI Damping Controller," *IEEE Access*, vol. 9, pp. 105641–105650, 2021.

[5] H. Wu, K. S. Tsakalis, and G. T. Heydt, "Evaluation of time delay effects to wide area power system stabilizer design," *IEEE Trans. Power Syst.*, vol. 19, no. 4, pp. 1935–1941, 2004.

[6] F. Wilches-bernal *et al.*, "Effect of Time Delay Asymmetries in Power System Damping Control," *IEEE Power Energy Soc. Gen. Meet.*, no. July, 2017.

[7] W. Zhou and et al, "Analysis of primary frequency regulation characteristics of PV power plant considering communication delay," *Energy Reports*, vol. 9, pp. 1315–1325, 2023.

[8] P. Zoghby, B. Marinescu, and A. Rosse, "A Conceptual Benchmark for the Study of Interactions and Inter-area Oscillations in Power Systems With High Power Electronics Penetration," *IEEE ISGT Eur.*, 2023.

[9] G. S. Pereira, "Stabilité des systèmes électriques comportant une forte proportion de sources interfacées par électronique de puissance," Ph.D. dissertation, Centrale Lille, 2020.

[10] V. Hanta and A. Procházka, "Rational approximation of time delay," 2014.

[11] G. Rogers, *Power system oscillations*. Springer Science + Business Media New York, 2000.

[12] Z. Liu and et al, "Effect analysis of generator governor system and its frequency mode on inter-area oscillations in power systems," *Int. J. Electr. Power Energy Syst.*, vol. 96, no. August 2017, pp. 1–10, 2018, [Online]. Available: https://doi.org/10.1016/j.ijepes.2017.09.034.

[13] C. Duggan, X. A. Liu, R. Best, P. Brogan, and J. Morrow, "Active power control from wind farms for damping very low-frequency oscillations," *Front. Energy Res.*, vol. 10, no. August, pp. 1–13, 2022, doi: 10.3389/fenrg.2022.962524.

[14] G. Sachin, "Small Signal Stability Analysis in Inverter Based Resource Dominated Power System," *Work. Gr. - CIGRE Study Comm. C4*, pp. 7–10, 2020.

[15] M. Belhocine and F. Xavier, "Input signal and model structure analysis for the HVDC link POD control," *IEEE PowerTech*, 2017.

[16] E. V. Larsen and D. A. Swann, "Applying power system stabilizers. Part I: General concepts," *IEEE Trans. Power Appar. Syst.*, vol. 3, no. September, pp. 3017–3024, 1981.

[17] E. V. Larsen and D. A. Swann, "Applying power system stabilizers. Part II: Performance objectives and tunning concepts," *IEEE Trans. Power Appar. Syst.*, no. 6, pp. 3025–3033, 1981.

[18] E. V. Larsen and D. A. Swann, "Applying power system stabilizers. Part III: Practical considerations," *IEEE Trans. Power Appar. Syst.*, no. 6, pp. 3034–3046, 1981.

[19] European Commission, "Commission Regulation (EU) 2017/1485: Establishing a guideline on Electricity Transmission System Operation (SO GL)," *Off. J. Eur. Union*, vol. L 220, no. 25 August 2017, p. 120, 2017.

[20] R. Leeraruji and M. Bollen, *Synthetic inertia to improve frequency stability and how often it is needed*. 2015.